

Preparation of Perfluorooctanoic acid Incorporate Nano size Poly (o-toluidine) And it's Characterization

B. Mahalakshmi ¹, C. Vedhi ²

¹ Department of Chemistry, V.O. Chidambaram College, Thoothukudi, India

² Affiliated to Manonmaniam Sundaranar University, Tirunelveli, TamilNadu, India

Abstract: - Perfluorooctanoic acid (PFA) doped poly (o-toluidine) (POT) was synthesized via chemical oxidative polymerization of o-toluidine with potassium peroxydisulphate as an oxidant. The role of doping on the structure and morphological changes in poly (o-toluidine) were characterized by FTIR, UV-Visible spectroscopy, cyclic voltammetric (CV), SEM, TGA, XRD, TEM and electrochemical impedance spectroscopy measurements and the results were analyzed. The solubility of perfluorooctanoic acid doped poly (o-toluidine) was studied in various solvents. It showed good solubility in DMSO, DMF, acetone, acetic acid, THF and Dichloromethane. The bands at 1765, 3326 and 1400 cm⁻¹ belonging to PFO are observed in the spectra of surfactant doped polymers. SEM analysis shows the change in the surface morphology of doped poly (o-toluidine) was predominantly dependent on the concentration of the surfactant. Elemental analysis was done by EDAX which shows the presence of C, N, O and F. XRD pattern showed that the formation of nanosized (39nm) polymer. Cyclic voltammetric studies of the surfactant doped polymer exhibited one oxidation peak at 376.3 and one reduction peak at -73.8 mV. Electrical conductivity of PFO doped POT increased with increase of the surfactant concentration. The X-ray diffraction (XRD) pattern and transmission electron microscopy (TEM) image showed that the formation of nano sized polymer.

Keywords

Poly (o-toluidine), Perfluorooctanoic acid, XRD, Cyclic Voltammetry, morphology.

1. INTRODUCTION

Conducting polymeric materials contain conjugated bonds have attracted much interest in scientific and technological areas in recent years. The unique optical, electrical and chemical properties offer these materials to be used in electronic displays, telecommunication, biosensors [1] anticorrosion coatings, rechargeable polymeric batteries, electromagnetic shielding, polymer photovoltaic's, polymer actuators [2, 3]. Among all conducting polymers, polyaniline is one of the most promising conducting polymers; but this is inherently brittle and has poor processibility, due to the insolubility in common organic solvents [4-6]. This problem has been overcome to some extent by using substituted derivatives of anilines such as o-toluidines, anisidines, N-methyl or N-ethyl anilines etc. [7-9]. In order to obtain additional insight into polyaniline, a methyl substituent has been used to block the ortho position of aromatic ring of aniline. It may be remarked that methyl-substituted aniline called o-toluidines has been found to have additional advantage over polyaniline due to its fast switching time between the oxidized and reduced states. POT was chosen as the conducting polymer owing to its higher processibility as well as solubility as compared with PANI [10]. Polymeric stabilizers (surfactant) affect the

polymerization condition, kinetics and also the final properties of the polymer [11, 12]. The role of non-ionic surfactants, e.g. those based on poly (ethylene oxide) and Triton X-100 (Tx-100) are less frequent and those dealing with cationic types are rare in the literature [13-15]. Suspension polymerization of aniline in the presence of dodecylbenzenesulfonic acid (DBSA) with styrene-butadiene-styrene (SBS) and without SBS was carried out and result indicates that DBSA acts simultaneously as a surfactant (emulsifier) and as a dopant [16, 17]. Also surfactant affect on the morphology (degree of crystalline order and orientation) [17]. Particle size and conductivity can be decreased by increasing the concentration of stabilizer [18, 19]. The surfactants influence the physical properties (morphology, solubility) of the resultant polymer [20]. The presence of surfactants improves the colloidal solubility of conducting polymers in organic solvents [21-23] and consequently, the processability [24, 25]. In the present paper, report the synthesis of POT-PFO by chemical oxidation polymerization in aqueous medium using KPS as an oxidant in the presence of various surfactant ratios. The effect of surfactant on POT, at different surfactant ratios and potential windows is investigated. FTIR studies have been performed to study

the structural changes due to the incorporation of dopant into polymeric chain. The surfactant changes the surface morphology of POT. It is also found that electrical conductivity of POT-PFO was better than that of undoped POT. This work is mainly focused on the contribution of perfluorooctanoic acid (PFO) micelles to the formation of stable dispersions of POT and characterization.

II. EXPERIMENTAL SECTION

2.1. Materials

Perfluorooctanoic acid (PFO, surfactant) and potassium peroxydisulfate (KPS, oxidant) were purchased from merck AR grade and used as such without further purification. (o-toluidine) was purified by distillation in vacuum before use.

2.2. Synthesis of polymer

PFO doped polymers were synthesized by keeping the concentration of the monomer (0.1 M) and the oxidant (0.1 M) constant and varying the molar ratio of PFO (below cmc). Table 1 describes the synthetic conditions of the respective samples. Bulk polymerization was carried out by mixing various molar ratio of surfactant into 2.3 ml of 0.1 M (o-toluidine) and made up to 250 ml using conductivity water. Polymerization was performed by (toluidine) the addition of potassium peroxodisulphate (0.1 M) in the micellar solution and stirred for 5 hrs. As the polymerization proceeded, the color of the solution changed to white through yellow, brown and finally to green, which indicates the formation of emeraldine salt (ES). The precipitated particles were collected after filtering and washing with distilled water then dried at room temperature.

2.3. Characterization

FT-IR spectra (model: SHIMADZU) of the polyaniline samples were recorded in the frequency range from 400 to 4000 cm^{-1} . UV-Vis spectra of the samples in DMSO were taken using JASCO-V530 dual beam spectrophotometer in the wavelength region 200 to 1100 nm with a scanning speed of 400 nm/min. X-ray diffraction patterns of the polymers were obtained by employing XPERT-PRO diffractometer using CuK_α ($k_\alpha = 1.54060$) radiation. The diffractometer was operated at 40 Kv and 30 mA. Powder X-ray diffraction pattern was recorded. The morphological study of the polymers were carried out using scanning electron microscope (SEM Model: JEOL JSM 6360) operating at 25 kV. The electrochemical workstation (model 650C), CH-Instrument Inc., TX, USA was employed for performing Cyclic voltammetry and impedance studies. The particles size were studied using TEM instrument (Model: PHILIPS-CM200) operating at 20–200 kv with a resolution of 2.4 Å. The percentage solubility of the polymers were determined by weight loss method (W/V %).

III. RESULTS AND DISCUSSION

3.1. Solubility

The solubility of perfluorooctanoic acid (PFO) doped poly (o-toluidine) was studied in various solvents. The solubility percentage of PFO doped polymers are presented in the table 2. The percentage of solubility increases with increasing the concentration of the surfactants. This behavior was more advantageous for further processing of doped POT.

3.2. IR spectra

The FT-IR spectra of the synthesized polymer in the presence and absence of surfactants are given in Fig.1. The FT-IR spectra of pure POT are shown in fig.1 (f). The skeletal vibrations of the aromatic rings show two bands at 1598 and 1498 cm^{-1} , which are attributed to C=C stretching vibrations of quinoid and benzoid ring respectively [26, 27]. The intensity of quinoid ring stretching vibrations relative to the intensity of benzoid ring stretching vibrations is considered to be a measure of the degree of oxidation of the polymer [28]. The intensity of the band at 1598 cm^{-1} is higher than that of the band at 1498 cm^{-1} indicating the presence of predominantly quinoid rings in POT (the polymer exit in its completely oxidized state) [28-30]. The shoulder at 1330 cm^{-1} and a weak peak at 1265 cm^{-1} are assigned to C-N stretching vibrations of quinoid and benzoid rings, respectively, as reported [31, 32]. The peak at 1265 cm^{-1} originates from the C-N stretching vibrations associated with the oxidation or protonation (doped) states in POT. The signal due to C-H in plane bending vibrations is observed at 1114 cm^{-1} . The peak at 879 cm^{-1} has been assigned to 1, 2, 4-trisubstituted aromatic rings indicating polymer formation [33]. The signal at 605 cm^{-1} is due to C-H out of plane bending vibrations. The new band appears at 1197 cm^{-1} which could be attributed to the $-\text{CH}_3$ rocking mode. The surfactant doped polymers have similar peaks of undoped POT but the stretching frequency values are shifted. The bands at 1765, 3326 and 1400 cm^{-1} belonging to PFO [34] are observed in the spectra of surfactant doped polymers. The relative intensity of these bands increases with increasing the surfactant content in the polymer. Hence FTIR shows surfactant well doped with the polymer.

3.3. UV-Vis spectra

The UV-Vis spectra of surfactant free and PFO doped POTs were recorded in DMSO and are shown in Fig. 2. The first absorption band appears in the region of 302-310 nm is assigned to the $\pi-\pi^*$ transition of the benzenoid ring. It is related to the extent of conjugation between the phenyl rings along the polymeric chain. The absorption band at 603 nm correspond to $n-\pi^*$ transitions and insulating pernigraniline phase of the polymer [35]. The absorbance band appears in the region of 805-817 nm assigned to polaron form (surfactant doped POT). The peak in the visible range also confirms the presence of doped state of conducting polymer. The band at around 346 nm is considerably blue shifted which indicates the interaction

between POT and the surfactant. The intensity of absorption band increases with the increasing PFO content.

3.4. SEM analysis

The SEM micrograph of PFO doped and undoped POT is shown in the fig.3. The SEM micrograph of undoped POT in Fig. 3(a) exhibits a granular structure [36]. Fig. 3(b) showed the tube like structure for POT 1. In the case of POT 2 showed globular structure (fig. 3(c)) with more pores in the polymer matrix and segregated spherical morphology (fig. 3(d)) is observed for POT 3. Fig. 3(e) depicts the granular structure for POT 4 and POT 5 showed the flower like structure shown in the fig. 3(f). The size and homogeneity of the particles are dependent on the type and concentration of surfactant. The variation in morphology of the doped POT was predominantly dependent on the concentration of the surfactant. Fig.4 Shows the EDS spectroscopy for the undoped and PFO doped POT. It can be seen from line a for the undoped POT, only peaks corresponding to C and N elements were displayed. While for the PFO doped POT, besides above peaks, peaks corresponding to C, N and F were also clearly observed, suggesting that F element originated from PFO was doped into the polymer.

3.5. XRD analysis

The results of X-ray diffraction are shown in Fig. 5. XRD patterns of surfactant doped samples show the semi-crystallinity (Figure 5). The concentration of the surfactant increases due to the increase in crystallinity of the sample. XRD patterns of undoped POT sample shows an amorphous hump around 24 $^{\circ}$ and the particle size is 53nm. The particle size of POT 1 is 39 nm, while in the case of POT 5 it is 74nm. Particle size and conductivity can be decreased by increasing the concentration of stabilizer. The variation in diffraction intensity with dopant concentration exhibits with the interaction of PFO in POT network.

3.6. Cyclic Voltammogram

Cyclic voltammograms of POT and PFO doped POT were recorded in the potential range from -0.6 to +1.2 V (Fig. 6). The surfactant free POT exhibit three oxidation peaks. The peak appeared at 992.2 mV corresponds to the oxidation of the monomer. The peak 279.4 mV was attributed to the transformation of POT from the reduced leucoemeraldine (LE) state to the partially oxidized emeraldine state (ES) of POT. The peak at 610.6 mV due to the presence of quinine/hydroquinone [37-39]. The surfactant doped POT also shows one redox peak around 376.3/-73.8 mV. The cathodic and anodic peak positions of PFO doped POT shifted and increases the peak current with increasing the concentration of the surfactant were shown in the curve from (e-a). This increase in current was due to fast redox process at POT-PFO matrix surface. As the scan rate increases the peak current of polymer increased linearly, indicating an adherent film on the glassy carbon electrode, was further confirmed by a straight line graph obtained by plotting peak current Vs scan rate as shown in Fig. 7.

3.7. Impedance spectra

The Nyquist plots of PFO doped and undoped POT in 0.1M H₂SO₄ are shown in fig.8. The diameter of the semi-circle gives an approximate value of the charge transfer resistance (R_{ct}) of the POT/electrolyte interface. The charge transfer resistances (R_{ct}) and C_{dl} values are presented in table 3. It can be observed that R_{ct} value increased with a decrease in surfactant concentration. The polymer doped with maximum PFO (POT 1) gives maximum conductivity

3.8. TGA/DTA

The thermo gravimetric analysis of POT and surfactants doped POT are shown in fig.9. It is generally known that three weight loss steps are observed in the TGA measurements for poly (o-toluidine) and surfactants doped POT. The thermo gravimetric analysis exhibits a three step loss in the range of 360C-702 0C for POT. The first weight loss starts from room temperature to 315oC corresponds to the loss of water molecule/moisture and dopant (HCl) present in the polymer matrix. The TGA curve does not show appreciable change in weight of sample up to 315 oC. The weight loss after 461.17 oC corresponds to degradation of the polymer backbone [40]. Fig. 9 (b) shows 32.5% weight loss (37.02 -162.47oC) is assignable to the loss of water molecules. In the second step (162.47-298.21oC), elimination of loosely bounded dopant (surfactant) is expected. The weight losses after 478.06 oC corresponds to degradation of the polymer backbone [41].

3.9. TEM

TEM images of surfactant doped POT is shown in the fig. 10. The figure shows that it is rod like structure and the particles were found to be in nano range. In the image the dark portion which is rod in nature are the surfactant and the grey areas is showing the polymer chain. Hence it is clear from the micrograph that the surfactant molecules are incorporate into the polymer.

IV. CONCLUSION

The absorption band in the region 805-817 nm indicates the doped state of POT. The FT-IR shows the peak at 1598 cm⁻¹ was shifted to 1589 cm⁻¹, which indicates the interaction between polymer and the surfactant. The SEM micrograph reveals distinct morphological features of PFO doped POT. EDAX confirmed the incorporation of PFO in POT. XRD results reveal that the high concentration of surfactant exhibit the particle size 39 nm and at low concentration of surfactant exhibit the particle size 74 nm. Electrochemical behavior was studied by CV and exhibit one oxidation peak at 376.3 mV and one reduction peak at -73.8 mV. The electrical conductivity was measured and POT 1 shows higher conductivity, which was confirmed by impedance spectra. The thermal stability of PFO doped POT is higher than that for the pure POT. TEM image confirmed the nano-sized particle.

V. ACKNOWLEDGMENTS

The authors were extremely grateful to DST (FAST TRACK and FIST) New Delhi, INDIA for using CHI Electrochemical workstation and JASCO UV-VIS spectrophotometer (UGC New Delhi) at V. O.Chidambaram College Tuticorin.

Table 1. Synthetic conditions of doped and undoped

Sample	o-toluidine(M)	KPS(M)	PFO(M)
POT	0.1	0.1	-
POT 1	0.1	0.1	1×10^{-2}
POT 2	0.1	0.1	1×10^{-3}
POT 3	0.1	0.1	1×10^{-4}
POT 4	0.1	0.1	8×10^{-5}
POT 5	0.1	0.1	2×10^{-5}

Table 2. The range of percentage solubility of PFO doped POT (POT 1 – POT 5) in various solvents

Solvent	% solubility
DMSO	100
DMF	100
Acetone	82-85
Aceticacid	76-79
Dichloromethane	71-76
THF	84-88
Water	30-34
Toluene	43-47
Xylene	40-45

Table 3. Impedance parameters of PFO doped and undoped POT

Polymer	$R_{ct}(\Omega cm^2)$	$C_{dl}(\mu F cm^{-2})$
POT (pure)	2297.8	0.0606
POT 1	390.4	2.3400
POT 2	445.6	1.7057
POT 3	980.8	0.3361
POT 4	1442.0	0.1566
POT 5	1666.8	0.1166

REFERENCES

[1] D. D. Borole, U. R. Kapadi, P. P. Mahulikar and D. G. Hundiwala, Journal of Material science, vol. 40, pp. 5499-5506, 2005.

[2] M. Atobe, A. N. Chowdhury, T. Fuchigami and T. Nonaka, Ultrasonics Sono chemistry, vol. 10, pp. 77, 2003.

[3] Jiping Yang and Bo Weng, Synthetic Metals, vol. 159, pp. 2249-2252, 2009.

[4] M. Angelopoulos, A. Ray, A. G. MacDiarmid and A. J. Epstein, Synth. Met., vol. 21, pp.12, 1987.

[5] A. Andreatta, Y. Cao, J. C. Chiang, A. J. Heeger and P. Smith, Synth. Met., vol. 26, pp. 383, 1988.

[6] N. Kumar, S. R. Vadera, J. Singh, G. Das, S. C. Negi, P. Aparna and A. Tuli, Def. Sci. J., vol. 56, pp. 91, 1996.

[7] L. H. Dao, M. Leclerc, J. Guay and J. W. Chevalier, Synth Met. E, vol. 29, pp. 377, 1989.

[8] D'Aparno, G. Leclerc, M and G. Zotti, J. Electroanal Chem., vol. 35, pp. 145, 1993.

[9] R.J. Mortimer, Electrochromic materials. Mater Chem., vol. 5, pp. 969, 1995.

[10] M. Datta and R. J. Singhal, Appl. Polym. Sci., vol. 103, pp. 3299, 2006.

[11] S.P. Armes and M. Aldissi, J. Chem. Soc., Chem. Comm., vol. 2, pp.88, 1989.

[12] N. Kohut-Svelko, S. Reynaud and J. Francois, Synth. Met., vol. 150, no. 2, pp. 107, 2005.

[13] D.Kim J. Choi, J-Y. Kim, Y-K Han and D. Sohn. Macromolecules, vol. 35no.13 pp. 5314, 2002.

[14] M. Omastov M. Trchova, J. Kovarova and J. Stejskal, Synth. Met., vol.138, no.3, pp.447, 2003.

[15] Z. Zhang, Z. Wei and M. Wan, Macromolecules, vol. 35, no.15, pp.5937, 2002.

[16] H. Q. Xei, Y.M. Ma and J.S. Guo, Polymer, vol. 40, no.1, pp. 261, 1998.

[17] J. E. Osterholm, Y. Cao, F. Klavetter and P. Smith, Polymer, vol. 35, no.13, pp. 2902, 1994.

[18] S.P. Armes, J. F. Miller and B. Vincent, J. Colloid Interface Sci., vol.118, no.22, pp.410, 1987.

[19] S.P. Armes and M. Aldissi, Polymer, vol. 31, no. 33, pp. 569, 1990.

[20] B. Sun, J.J. Jones, R.P. Burford and M. Skyllas-Kazacos, *J. Mater. Sci.*, vol. 24, no.11, pp.4024, 1989.

[21] P.J. Kinlen, B. G. Frushour, Y. Ding and V. Menon, *Synth. Met.*, vol. 101, pp.758, 1999.

[22] M. Wan, J. Huang and Y. Shen, *Synth. Met.*, vol. 101, pp. 708, 1999.

[23] A.J. Dominis, G. M. Spinks, L. A. P. Kane-Maguire and G. G. Wallace, *Synth. Met.*, vol. 129, pp. 165, 2002.

[24] D. Ichinohe, T. Arai, and H. Kise, *Synth. Met.*, vol.84, pp.75, 1997.

[25] E. J. Oh, K. S. Jang and A. G. MacDiarmid, *Synth. Met.*, vol. 125, pp. 267, 2002.

[26] J. Tang, X. Jing, B. Wang and F. Wang, *Synth. Met.*, vol. 24, pp. 231, 1988.

[27] Z. Ping, H. Neugebauer and A. Neckel, *Electrochim. Acta*, vol. 41, pp. 767, 1996.

[28] N. S. Sariciftci, H. Kuzmany, H. Neugebauer and A. Neckel, *J. Chem. Phys.*, vol. 92, pp.4530, 1990.

[29] Z. Ping, *J. Chem. Soc. Faraday Trans.*, vol. 92, pp. 3063, 1996.

[30] N. Chandrakanthi and M. A. Careem, *Polym. Bull.*, vol. 45, pp. 113, 2000.

[31] D. Shan and S. Mu, *Synth. Met.*, 2002, 126, 225.

[32] T. C. Wen, L. M. Huang and A. Gopalan, *Synth. Met.*, vol. 123, pp. 451, 2001.

[33] M. S. Wu, T. C. Wen and A. Gopalan, *Mater. Chem. Phys.*, vol. 74, pp. 58, 2002.

[34] Sara DalleVacche, Valerie Geiser, Yves Leterrier and Jan-Anders E. Manson, *Polymer*, vol. 51, pp. 334, 2010.

[35] A.J. Heeger, S. Kivelson, J. R. Schrieffer and W. P. S., *Rev. Mod. Phys.*, vol. 60, pp. 781, 1988.

[36] M. Kulkarni and A. Viswanath, *J. Macromol. Sci. A*, vol. 41, pp. 1173, 2004.

[37] D.D. Borole, U. R. Kapadi, P.P Mahulikar and D. G. Hundiware, *J. Appl. Poly. Sci.*, vol. 90, pp. 2634, 2003.

[38] D.E. Stilwell and S. M. Park, *J. Electrochem. Soc.*, vol. 135, pp. 2254, 1988.

[39] B.J. Johnson and S. M. Park, *J. Electrochem. Soc.*, vol. 143, pp. 1277, 1996.

[40] S.H. M. Ebrahim and A. Gad Morsy, *Synth. Met.*, vol. 160, pp. 2658, 2010.

[41] J. Anand, S. Palaniappan and D. N. Sathyanarayana, *Synth. Met.*, vol. 82, pp.23, 1996.

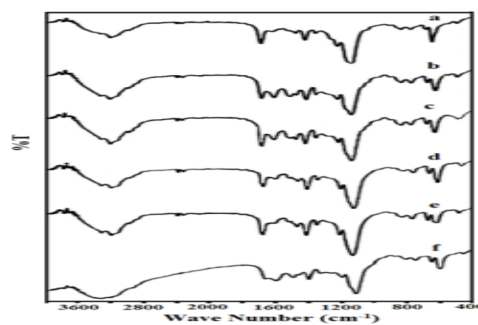


Fig.1. FT-IR spectra of a) POT 1 b) POT 2 c) POT 3 d) POT 4 e) POT 5 f) POT (undoped)

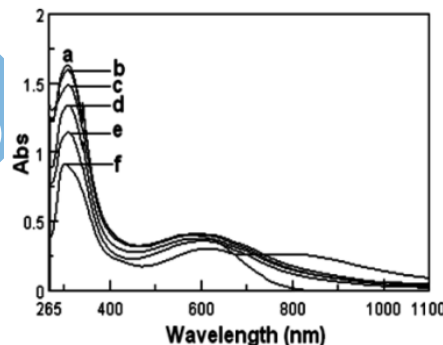


Fig.2. UV-Vis spectra of a) POT 1 b) POT 2 c) POT 3 d) POT 4 e) POT 5 f) POT (undoped)

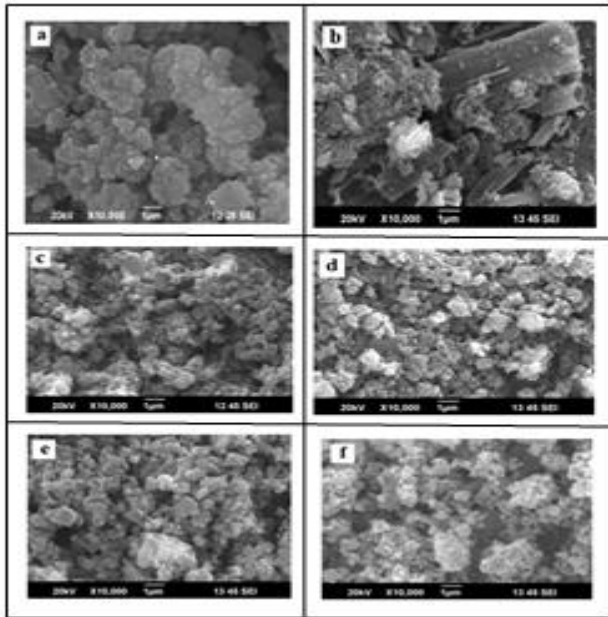


Fig.3. SEM photographs of a) POT (undoped) b) POT 1 c) POT 2 d) POT 3 e) POT 4 f) POT 5

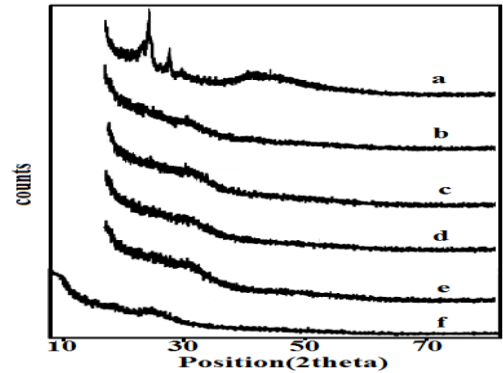


Fig.5. XRD of a) POT 1 b) POT 2 c) POT 3 d) POT 4 e) POT 5 f) POT (undoped)

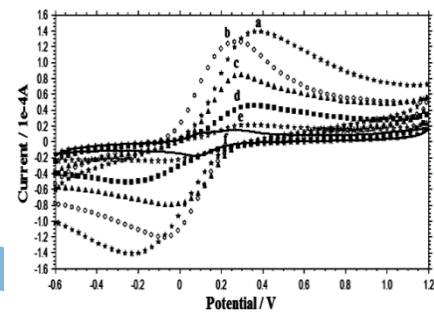


Fig.6. Cyclic voltammogram of a) POT 1 b) POT 2 c) POT 3 d) POT 4 e) POT 5 f) POT (undoped)

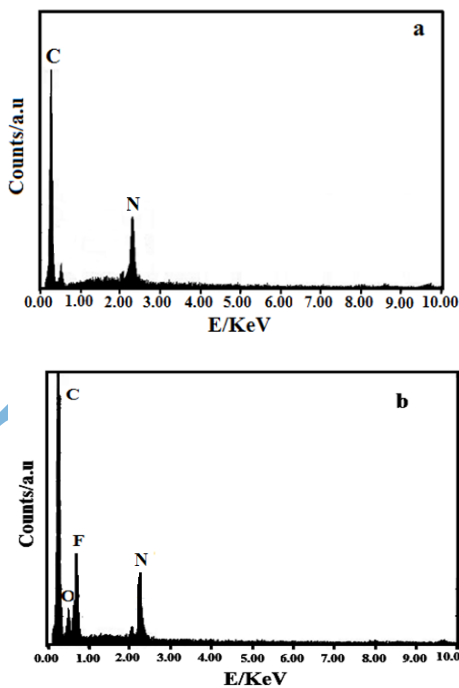


Fig.4. EDAX behaviour of a) POT (undoped) b) POT 1

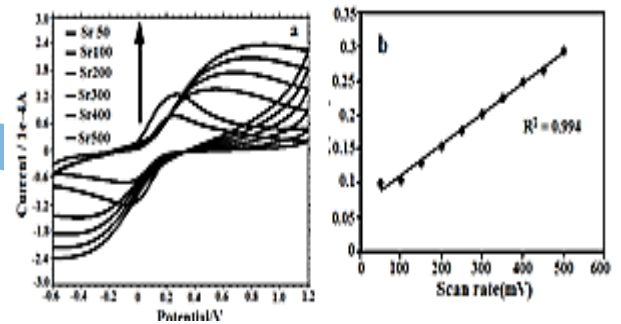


Fig.7. a) CV taken at various scan rates for POT 1 b) Plot of anodic current Vs scan rate for POT 1

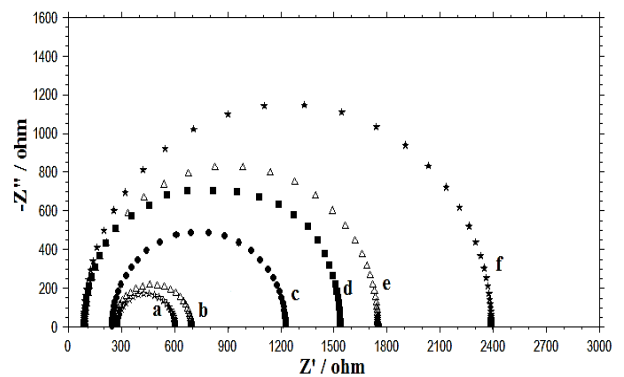


Fig.8. Impedance spectra of a) POT 1 b) POT 2 c) POT 3 d) POT 4 e) POT 5 f) POT (undoped)

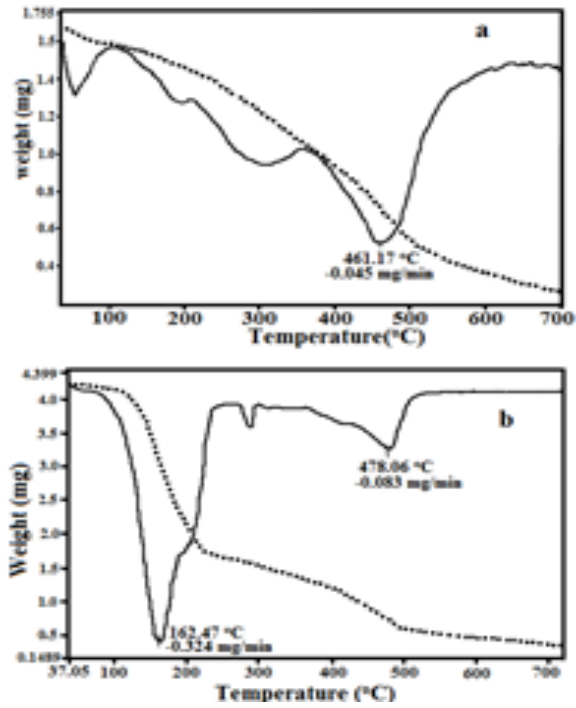


Fig.9. TGA/DTA images of a) POT (undoped) b) POT 1

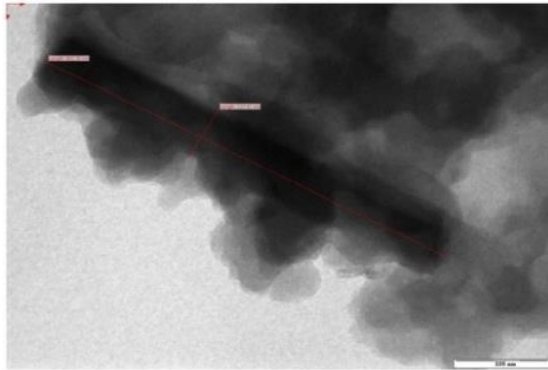


Fig.10. TEM image of POT 1